doi:10.1017/S1431927617004561
Microsc. Microanal. 23 (Suppl 1), 2017

Correlated EBSD and High Speed Nanoindentation Mapping

Eric Hintsala[1], Jared Risan[1], Robert Dietrich[1] and Richard Nay[1]

[1.] Bruker Corporation, Bruker Nano Surfaces Division, Minneapolis, MN

Nanoindentation techniques have long had an important role in evaluating the mechanical properties of microstructural features. In recent years, high speed nanoindentation mapping techniques have been under development and have recently achieved speeds up to 6 indents/second. This gives speed, resolution and scan size comparable to that of electron backscatter diffraction (EBSD), allowing for one-to-one correlation techniques with corresponding large data sets for statistical analysis. This correlation can produce high resolution structure-property (EBSD: structure, nanoindentation:property) relationships which can be mapped over length scales of several microns to several hundreds of microns. This has numerous potential applications, from evaluation of microstructural evolution during processing [1], quality control testing of weld zones [2], evaluation of sub-surface damage gradients [3] (wear, corrosion, irradiation), composite material interfaces [4] and more.

In this study, a 410L stainless steel laser cladding deposited on a 4140 steel substrate is explored. This material is deposited through laser sintering of metallic powder to give a cost-effective corrosion and wear resistant coating. The steels are similar in that they are ferritic and martensite-hardened, but the 410L possesses ~10%Cr content to produce a passivation layer, which increases the cost. The hardness of the cladding, weld zone and heat affected zone in the 4140 substrate need to be carefully controlled to ensure machinability and reliability of the final component.

A mounted and polished cross section was examined in an FEI Versa FIB/SEM to identify the cladding substrate interface. A fiduciary box (Fig. 1B) was patterned with the focused ion beam around the area of interest. The was mapped using an EDAX Hikari EBSD detector at 20kV accelerating voltage and 0.2 µm step size. The nanoindentation map was produced using the accelerated property mapping (XPM) mode of a Hysitron TI-980 Triboindenter equipped with a diamond Berkovich tip. For the XPM maps, a constant force of 400 µN was utilized with an indent spacing of 500nm over a 34 x 34 µm area (N = 4356 indents).

The nanoindentation modulus map shown in Fig. 1A shows a fairly constant value (218.5 ± 17.5 GPa) as expected. The interface of the two materials can be clearly identified from the hardness map (Fig. 1C), with an average value of approximately 5 GPa for the 4140 and 8 GPa for the 410 cladding. From the EBSD inverse pole figure in Fig. 2B some differences between the materials can be seen, where the orientation varies more strongly spatially in the clad compared to the substrate. This is also apparent when examining the boundary map in Fig. 2A, where there is a dense network of high angle grain boundaries within the clad. There is also definitive hardness “hot spots” within the 410 cladding. It seems reasonable that the higher average hardness and the appearance of hardness hotspots is related to this increased boundary density.

The metals joined in this study were found to produce a fairly uniform interface, however, this data could be utilized further to optimize processing through adjustments of laser settings or by experimenting with different material combinations. This should be even more critical in the case of

bonding dissimilar metals together, where intermetallic phases of extremely high hardness and low ductility could form and serve as initiation points for fracture.

References:

[1] I. S. Wani, T. Bhattacharjee, S. Sheikh, I. T. Clark, M. H. Park, T. Okawa, S. Guo, P. P. Bhattacharjee and N. Tsuji, N., Intermetallics **84** (2017) pp.42-51.
[2] V. H. B. Hernandez, S. K. Panda, Y. Okita and N. Y. Zhou, J. Mater. Sci. **45** pp.1638-1647.
[3] R. Kasada, Y. Takayama, K. Yabuuchi and A. Kimura, Fusion Engineering and Design **86** (2011) pp.2658-2661.
[4] M. Campo, A. Urena and J. Rams, Scripta materialia **52** (2005) pp.977-982.

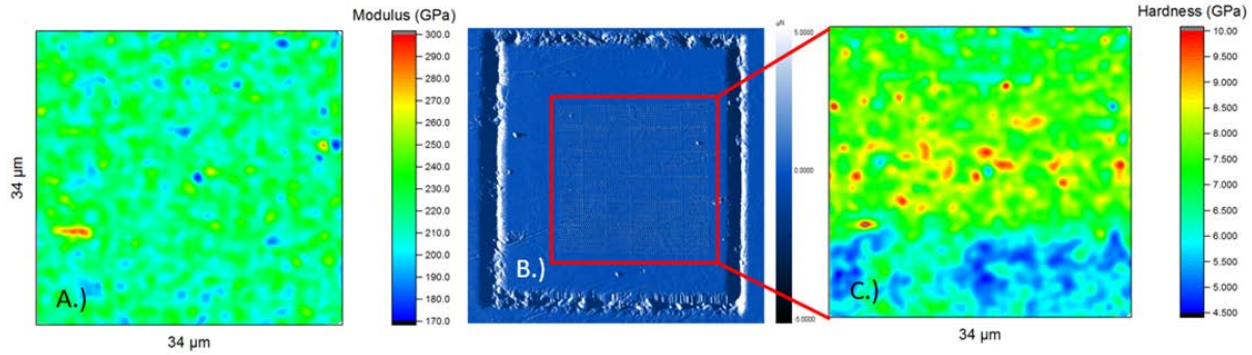

Figure 1. Nanoindentation maps of the area of interest, with A.) modulus, B.) optical micrograph showing the FIB marked box and indentation grid and C.) hardness.

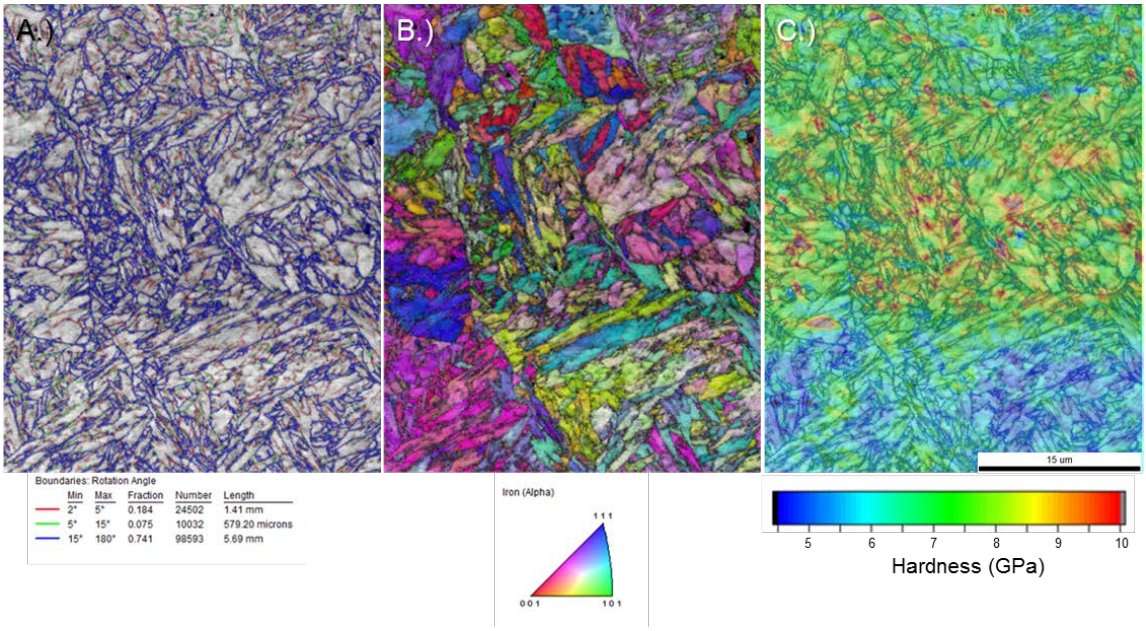

Figure 2. EBSD map of the area of interest with A.) image quality map with grain boundaries overlaid, B.) inverse pole figure map for the iron alpha (ferrite) phase and C.) Hardness map from Fig. 1 overlaid on the boundary map from (A.)

https://doi.org/10.1017/S1431927617004561 Published online by Cambridge University Press